EUROPEAN TRANSACTIONS ON ELECTRICAL POWER
Euro. Trans. Electr. Power 2009; **19**:509–517
Published online 5 March 2008 in Wiley InterScience
(www.interscience.wiley.com) DOI: 10.1002/etep.238

Measurement and simulation of the electric field of high voltage suspension insulators

Vassiliki T. Kontargyri, Ioannis F. Gonos*,† and Ioannis A. Stathopulos

High Voltage Laboratory, Electric Power Department, School of Electrical and Computer Engineering, National Technical University of Athens, 9, Iroon Politechniou Str., 15780 Zografou, Athens, Greece

SUMMARY

In this study, a method for the calculation of the electric field on high voltage insulators is presented. A model of the insulator string was set up using OPERA, an electromagnetic analysis program based on the Finite Element Method. In order to validate the accuracy of the method, simulated results have been compared with experimental results. Copyright © 2008 John Wiley & Sons, Ltd.

KEY WORDS: Insulators; electric field distribution; simulation software; finite element method

1. INTRODUCTION

The insulator strings, which are used for the suspension of overhead transmission lines, constitute one of the most important parts of the transmission lines as they used to give support to electrical conductors and shield them from ground or other conductors as well as they provide the necessary mechanical supports for the transmission lines against the worst likely mechanical loading conditions. The number of the insulator units that consists the suspension insulator string depends on the operating voltage of the overhead transmission line.

The calculation of the electric field and voltage distribution within and around high voltage insulators is a very important parameter for the design of the insulators. High levels of the electric field are possibly responsible for audible noise, electromagnetic pollution, partial discharge and premature aging of insulation. The assignment of the electric field distribution in an insulator string is useful as it is an indication for flashover propagation. Hampton's criterion shows that flashover cannot occur if the surface electric gradient is sufficiently low [1]. The flashover effects in insulators can cause the breakdown of a transmission system. Furthermore, the knowledge of the electric field is helpful for the detection of defects in insulators [2].

Several methods such as finite difference method [3], boundary element method [4–6] and finite element method [7–13] have been developed for the computation of electric fields and potentials along an insulator string. The simulation methods give the possibility to examine the behaviour of models with very complex geometry without using analytical methods or experiments. The electric field measurement along the insulator can also be found in many previous literatures such as references [6,14].

In this paper, the electric field distribution of a high voltage suspension insulator has been measured. In addition, the electric field and potential distribution around and inside the insulator when it is stressed by power frequency voltage is examined using OPERA, which is a suite of programs for two and three dimensional electromagnetic field analysis [17]. The software package uses the finite element method to solve the partial differential equations that describe the behaviour of electromagnetic fields. The critical points affecting simulation accuracy are examined and the simulated results are compared with experimental results.

*Correspondence to: Ioannis F. Gonos, High Voltage Laboratory, Electric Power Department, School of Electrical and Computer Engineering, National Technical University of Athens, 9, Iroon Politechniou Str., 15780 Zografou, Athens, Greece.
†E-mail: igonos@ieee.org

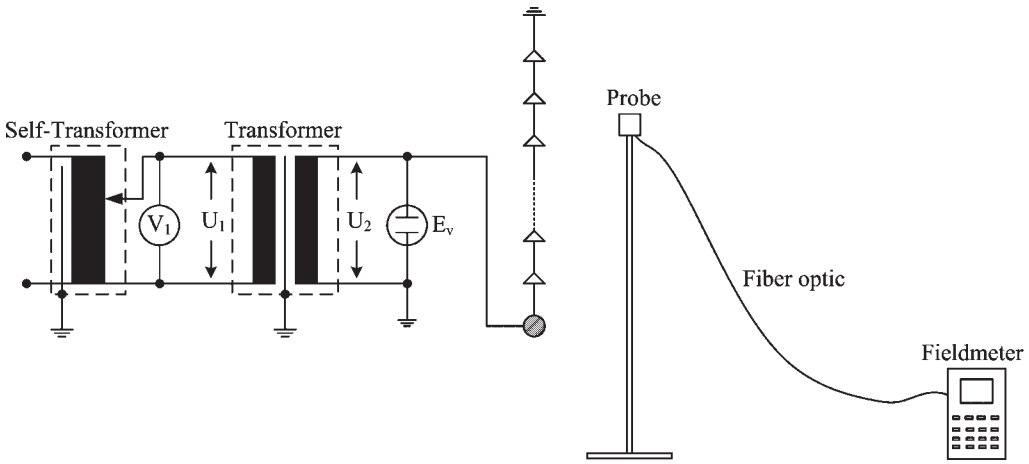

Figure 1. Experimental set-up used for the measurement of the voltage distribution.

2. EXPERIMENTAL PROCEDURE

The aim of the experiments was the study of the electric field distribution on the insulator string. The test arrangement for the measurement of the electric field is shown in Figure 1.

It includes a 230 V self-transformer. Through this self-transformer, a 110 V/55 kV transformer is fed. The voltage is measured by two methods. The first method is using the voltmeter V_1 in the primary part of the transformer and then transforming the low voltage U_1 in high voltage multiplying by the voltage transformer ratio (a). The second method is using an electrostatic voltmeter E_v and measuring the high voltage U_2 in the secondary part of the transformer [15,16]. The average U_t of the two values is the voltage applied across the ten-insulator string:

$$U_{ti} = \frac{U_{1i} \cdot a + U_{2i}}{2} \tag{1}$$

In order to measure the electric field around the insulator string the fieldmeter PMM 8053A and the probe PMM EHP 50B, which are connected via an optic fibre, were used, as shown in Figure 1. The probe was placed in different positions of the horizontal plane, while by the use of successive tubes, measurements were taken in many points of the perpendicular axis.

The height of the conductor is considered the reference point for the measurements. In the horizontal plane the *X*-axis is parallel to the HV conductor and the *Y*-axis is perpendicular to the conductor. The point (0,0) is the point where the *Z*-axis (that is the axis of the insulator string) intersects the horizontal plane. The electric field was measured in 11 positions of the horizontal plane and in 28 points in each position. In Figure 2 the coordinates of the 11 positions are shown. The insulator is suspended vertically at the point (0,0) of the horizontal plane.

3. EXPERIMENTAL RESULTS

The three components of the electric field E_x, E_y and E_z were measured. The total value of the electric field E_t was calculated according to the following equation

$$E_t = \sqrt{E_x^2 + E_y^2 + E_z^2} \tag{2}$$

The measurements of the electric field in the 11 positions shown in Figure 2 around the insulator string are presented in Table I. It is noted that the numbering of the *Z*-axis, that is the axis of the insulator string starts from the transmission line. In the points nearer the transmission line the electric field has higher values than in the points far from the transmission line.

DOI: 10.1002/etep

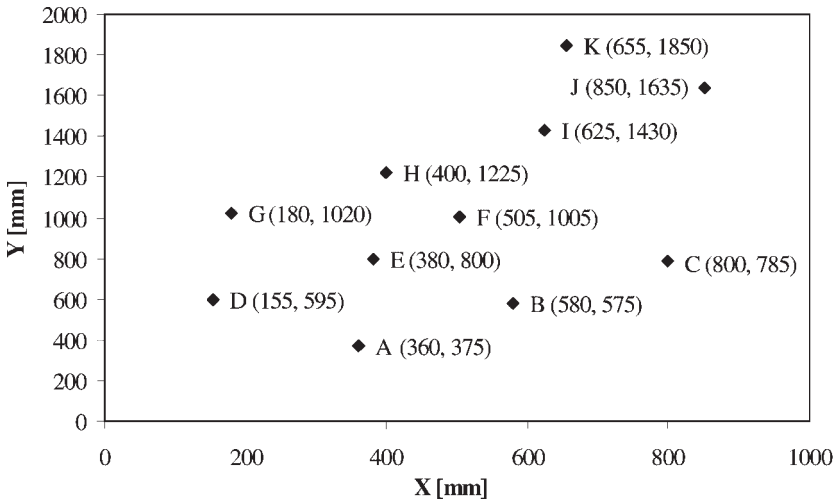

Figure 2. Locations in the horizontal plane where series of measurements of the electric field were carried out.

Table I. Experimental results of the electric field.

Z (cm)	Electric field (kV/m)										
	A	B	C	D	E	F	G	H	I	J	K
11.0	14.670	9.273	6.796	10.580	6.660	4.443	4.576	3.284	2.629	1.964	1.602
16.5	13.530	8.839	6.494	10.290	6.455	4.327	4.460	3.237	2.598	1.943	1.579
22.0	12.290	8.383	6.222	9.913	6.358	4.281	4.428	3.220	2.536	1.909	1.568
27.5	11.390	7.998	5.953	9.389	6.107	4.118	4.275	3.155	2.495	1.880	1.551
33.0	10.450	7.518	5.626	9.014	5.821	4.004	4.208	3.078	2.473	1.852	1.510
38.5	10.090	7.092	5.389	8.585	5.607	3.832	4.088	2.998	2.394	1.847	1.487
44.0	8.998	6.730	5.098	8.050	5.424	3.706	3.911	2.894	2.300	1.801	1.481
49.5	8.701	6.334	4.877	7.641	5.194	3.569	3.835	2.839	2.296	1.756	1.443
54.5	8.284	6.041	4.628	7.233	4.982	3.447	3.763	2.727	2.282	1.721	1.430
60.0	7.676	5.688	4.373	6.731	4.750	3.330	3.673	2.632	2.203	1.668	1.412
65.5	7.189	5.443	4.200	6.403	4.534	3.178	3.437	2.544	2.121	1.626	1.370
71.0	6.825	5.162	3.935	5.977	4.301	3.066	3.290	2.442	2.078	1.585	1.340
76.5	6.334	4.770	3.757	5.637	4.089	2.888	3.144	2.377	1.988	1.534	1.303
82.0	5.894	4.467	3.517	5.283	3.834	2.778	3.021	2.300	1.924	1.488	1.236
87.5	5.560	4.236	3.352	5.009	3.651	2.645	2.886	2.205	1.852	1.433	1.235
93.0	5.202	3.976	3.193	4.667	3.437	2.500	2.748	2.092	1.777	1.375	1.208
98.5	4.839	3.777	2.995	4.362	3.266	2.387	2.589	1.994	1.732	1.335	1.165
104.0	4.514	3.560	2.836	4.036	3.080	2.312	2.445	1.889	1.672	1.304	1.115
109.5	4.254	3.354	2.671	3.813	2.898	2.208	2.337	1.830	1.589	1.251	1.071
115.0	3.937	3.113	2.536	3.519	2.717	2.092	2.214	1.745	1.535	1.214	1.056
120.5	3.666	2.952	2.411	3.312	2.567	1.992	2.005	1.667	1.465	1.163	1.019
126.0	3.407	2.763	2.295	3.124	2.407	1.860	1.989	1.582	1.416	1.118	0.992
131.5	3.206	2.611	2.174	2.882	2.329	1.766	1.925	1.519	1.347	1.078	0.954
137.0	2.972	2.433	2.054	2.703	2.142	1.601	1.826	1.424	1.301	1.041	0.925
142.5	2.791	2.310	1.951	2.534	2.021	1.610	1.708	1.373	1.263	1.004	0.895
148.0	2.590	2.171	1.847	2.337	1.926	1.508	1.567	1.316	1.189	0.960	0.861
153.5	2.399	2.028	1.730	2.176	1.812	1.435	1.525	1.244	1.143	0.928	0.830
159.0	2.261	1.874	1.651	2.033	1.690	1.347	1.395	1.178	1.095	0.895	0.798

DOI: 10.1002/etep

4. SIMULATION PROCEDURE

The suite of programs for two and three dimensional electromagnetic field analysis, OPERA, uses the finite element method (FEM) to solve the partial differential equations (Poisson's, Helmholtz and Diffusion equations) that describe the field [17]. The FEM is used to obtain solutions to partial differential or integral equations that cannot be solved by analytic methods. For the aim of this paper, the electromagnetic field analysis program TOSCA has been used. The TOSCA algorithm is based on Scalar Potential Formulation. Three dimensional stationary electromagnetic fields can be represented as the sum of a solenoidal field and a rotational field. In electrostatic fields there is never a rotational component, the field can therefore always be defined using the electrostatic potential (U). The electric field intensity ($\mathbf{E}$) is given by:

$$\mathbf{E} = -\nabla U \tag{3}$$

The divergence of the electric flux density ($\mathbf{D}$) is related to the charge density (ρ):

$$\nabla \mathbf{D} = \rho \tag{4}$$

Combining Equations (3) and (4) and introducing the dielectric permittivity tensor (ε) gives the usual Poisson's equation description of the electrostatic potential:

$$\nabla \cdot \varepsilon \nabla U = -\rho \tag{5}$$

where $D = \varepsilon E$.

In order to define U, boundary conditions are required, these may be either assigned values of U or its derivative.

A similar equation arises for current flow problems,

$$\nabla \cdot \sigma \nabla U = 0 \tag{6}$$

where σ is the conductivity, and $\mathbf{J} = \sigma \mathbf{E}$.

5. MODEL CONFIGURATION

The investigated suspension insulator string consists of 12 disc-shaped insulator units of toughened glass that are known as insulators of the cap and pin type and is used for the suspension of 150 kV overhead transmission lines crossing coastal and industrial areas, with remarkably high pollution. The first insulator unit is placed near the tower and the twelfth is placed near the transmission

(a) (b)

Figure 3. Views of the three dimensional model in Opera-3d.

DOI: 10.1002/etep

line. The geometrical characteristics of each insulator unit are the diameter, which is 280 mm, the height, which is 146 mm and the creepage distance, which is 430 mm.

A section of the transmission line is included in this model. The length of the conductor included in the model was set to be approximately equal with the length of the insulator string [6]. The conductor is sited along the *X*-axis while the insulator string is sited along the *Z*-axis, as shown in Figure 3(a). In Figure 3(b) the insulator unit is presented in details.

In the model, the density of the finite elements is higher in the critical regions of the insulator where higher accuracy is required and the electric properties of the materials are such that the electric field intensity changes rapidly. The total number of elements, that is 3 806 273, allows the accurate solution of the differential equations.

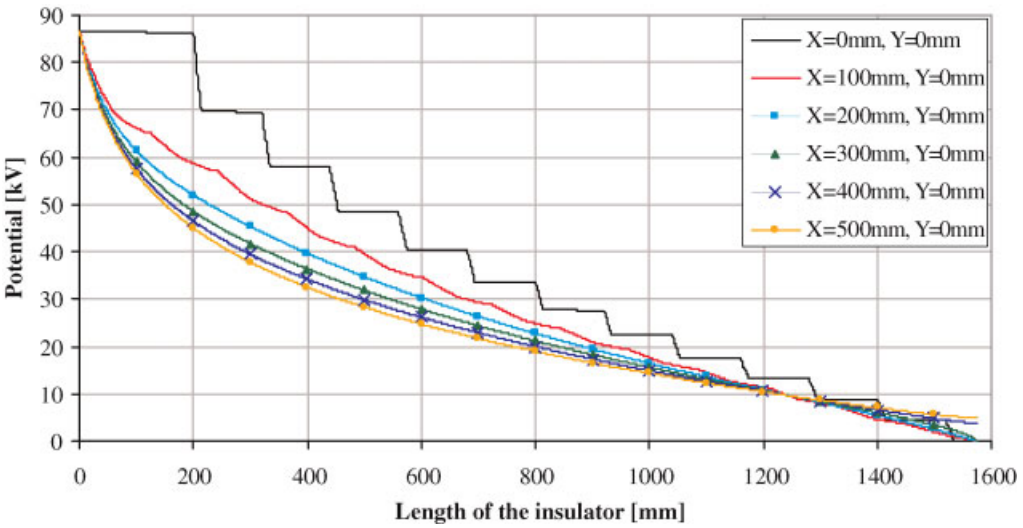

Figure 4. Potential along lines parallel to the insulator string and vertical to the conductor (*X*-axis).

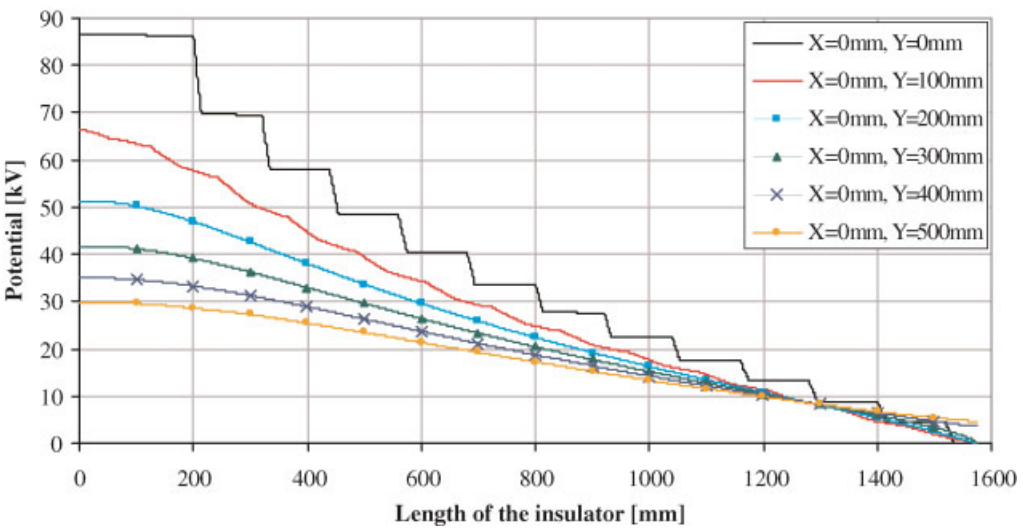

Figure 5. Potential along lines parallel to the insulator string and vertical to the *Y*-axis.

DOI: 10.1002/etep

The relative permittivity of the materials and the boundary conditions are assigned in the model. It is considered that the relative permittivity of the glass and the cement is 7 and 14, respectively. The value of the electric potential on the surface of the conductor is equal to $150/\sqrt{3}$kV, while the value of the electric potential on the surfaces of the parallelepiped that simulates the earth (tower) is equal to zero. In addition, the value of the electric potential on the external surfaces of the background is equal to 0 V, as it is assumed that the electric potential in the infinity is zero.

Although the number of the equations (933 597) is large due to the large number of the elements (3 806 273), the required time for solving the model is reduced in 19 minutes using a Pentium IV processor (3 GHz).

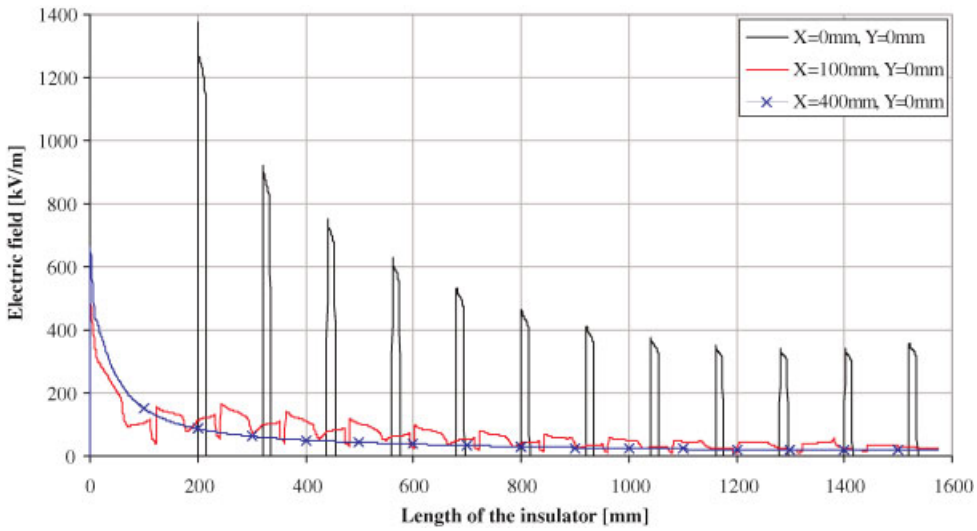

Figure 6. Electric field along lines parallel to the insulator string and vertical to the conductor (*X*-axis).

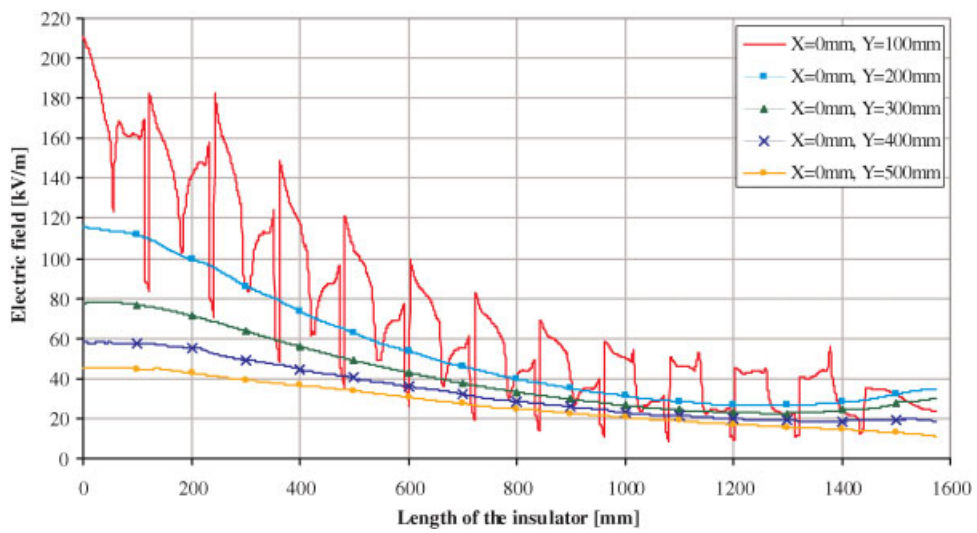

Figure 7. Electric field along lines parallel to the insulator string and vertical to the *Y*-axis.

DOI: 10.1002/etep

6. FEM RESULTS

Figure 4 represents the potential distribution along a set of lines running parallel to the axis of the insulators (*Z*-axis) and at different distances from it. The above lines are sited in the *XZ*-plane and they are vertical to the conductor (*X*-axis). The step-variation of the potential referred to the line that passes through the axis of the insulator string ($X = 0$ mm, $Y = 0$ mm) is due to the presence of the conducting parts of the insulator string.

Figure 5 illustrates the potential distribution along a set of lines running parallel to the *Z*-axis and perpendicular to the *Y*-axis (away from the conductor). The above lines are sited in the *YZ*-plane.

The electric field distribution along lines that are located in the *XZ*-plane and they are vertical to the *X*-axis is shown in Figure 6. The electric field along the line that passes through the axis of the insulator string ($X = 0$ mm, $Y = 0$ mm) is zero in the conducting parts of the insulator string and takes high values in the insulator and the cement. In Figure 7 the electric field along lines that are sited in the *YZ*-plane and they are vertical to the *Y*-axis is presented.

The electric field strength along the lines ($X = 100$ mm, $Y = 0$ mm) and ($X = 0$ mm, $Y = 100$ mm) passing through the insulator units of the insulator string, goes abruptly down when the line passes through the glass due to the bigger value of the permittivity of the glass in comparison to the permittivity of the surrounding air. As a result, there is a significant decrease in the electric field strength in the region of glass.

Comparing the values of the potential and the electric field that have been arisen from Figures 4 and 6 with the respective values of Figures 5 and 7, the potential and the electric field levels of Figures 4 and 6 are higher as the lines are sited nearer the excited conductor. This variation in the field around the azimuth of the insulator strings is the reason that it cannot be calculated using a two dimensional model and the development of a three dimensional model is necessary.

The potential distribution on a cartesian patch on the *YZ*-plane passing through the centre of the insulator string is presented in Figure 8 via coloured regions around the insulator string. It is clear that in a region close to the conductor, the potential is equal to $150/\sqrt{3}$kV, as expected, and gradually decreases.

7. COMPARISON BETWEEN EXPERIMENTAL AND SIMULATED RESULTS

The electric field simulated results were compared with the experimental results for seven indicative positions of the horizontal plane, A, B, E, G, I, J and K. The results of the comparison are shown in Figure 9.

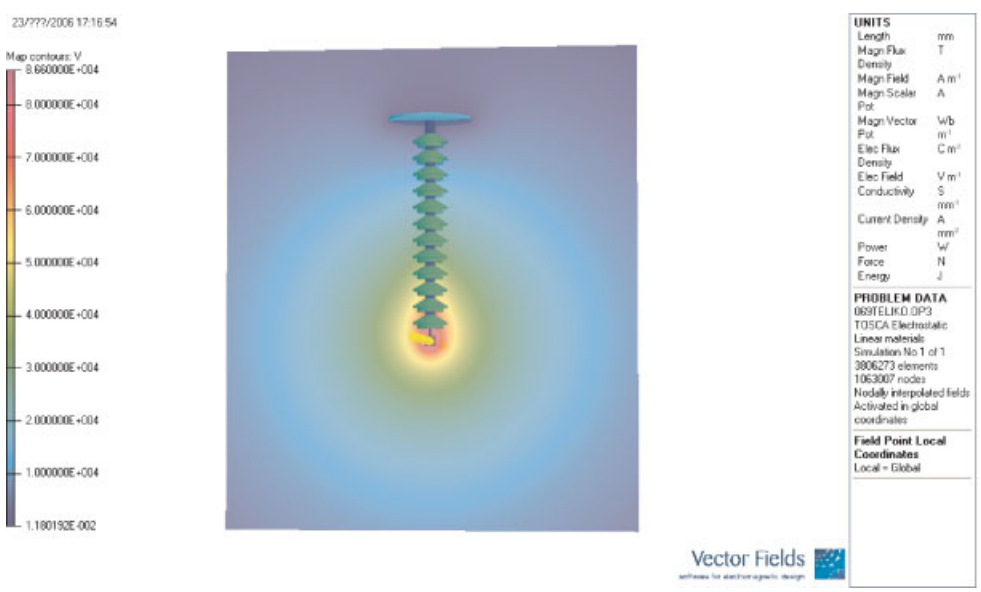

Figure 8. Zone map on a *YZ*- patch for the representation of the potential distribution around the insulator string.

DOI: 10.1002/etep

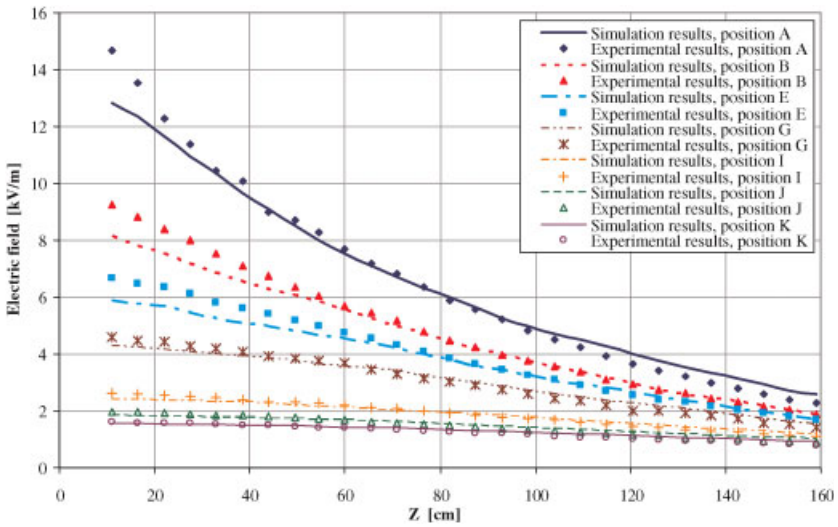

Figure 9. Comparison of the electric field distribution between the simulation and the experimental results in positions A, B, E, G, I, J and K.

A very good agreement has been ascertained, by comparing the experimental results for the electric field with the simulated results.

The mean square error m was calculated by the equation

$$m = \sqrt{\sum_{i=1}^{N} \left(\frac{1}{N} \left(\frac{E_{si} - E_{ei}}{E_{ei}} \right)^2 \right)} \tag{7}$$

where E_{si} is simulation value of the percentage of the voltage that is applied in the i-insulator and E_{ei} is the corresponding experimental value.

For the measurements at the position B the mean square error m is 5.16 and the maximum error between the simulation and the experimental results is lower than 12%. The mean square error m for the measurements at position I is 4.98 and the maximum error between the simulation and the experimental results is lower than 8%.

8. CONCLUSIONS AND DISCUSSION

In this paper the electric field distribution of a glass insulator string has been computed using the FEM. The three dimensional model of the insulator string including a part of the transmission line has been finely designed in order to increase the accuracy of the simulation procedure. High accuracy of the results obtained dividing the domain into a large number of finite elements and increasing the density of the elements in the critical regions of the insulator string. Although the complication of the problem the required time for solving the differential equations is limited. A very good agreement has been ascertained, by comparing the experimental results with the results from simulation. Taking into account that most of the times there are not the equipment or the place for experiments, the authors propose the simulation of the insulator string, which is an easy procedure and gives also accurate results. The studied approach is applicable to any insulator type, leading to reliable results in a very fast and economic way, helping the HV overhead line planners to the selection of the right insulator type.

9. LIST OF SYMBOLS AND ABBREVIATIONS

D electric flux density
E electric field intensity

DOI: 10.1002/etep

E_e experimental value of the percentage of the voltage that is applied in the insulator
E_s simulation value of the percentage of the voltage that is applied in the insulator
E_t total electric field
E_x X-component of the electric field
E_y Y-component of the electric field
E_z Z-component of the electric field
$\mathbf{J}$ current density
m mean square error
U electrostatic potential
U_t voltage applied across the insulator string
U_1 low voltage in the first part of the transformer
U_2 high voltage in the secondary part of the transformer
α voltage transformer ratio
ρ charge density
σ conductivity
ε dielectric permittivity tensor
FEM finite element method

ACKNOWLEDGEMENTS

The authors want to express their sincere gratitude to the Vector Field Company and especially to Dr. A. M. Michaelides for their kind support in the simulations. In addition, this project is co-funded by the European Social Fund (75%) and National Resources (25%)–Operational Program for Educational and Vocational Training II (EPEAEK II) and particularly by the Program HERAKLEITOS.

REFERENCES

1. Looms JST. *Insulators for High Voltages*. Peter Peregrinus Ltd.: London, UK, 1990.
2. Power Systems Research Center. Evaluation of critical components of non-ceramic insulators (NCI) In-Service: Role of defective interfaces; *Final Project Report*, PSERC Publications 04-32, Arizona, August 2004.
3. Morales N, Asenjo E, Valdenegro A. Field solution in polluted insulators with non-symmetric boundary conditions. *IEEE Transactions on Dielectrics and Electrical Insulation* 2001; **8**(2):168–172.
4. Rasolonjanahary JL, Krähenbühl L, Nicolas A. Computation of electric fields and potential on polluted insulators using a boundary element method. *IEEE Transactions on Magnetics* 1992; **38**(2):1473–1476.
5. Que W. A Electric field and potential distributions along non-ceramic insulators; Ph.D. Thesis, Department of Electrical Engineering, The Ohio State University, 2002.
6. Zhao T, Comber G. Calculation of electric field and potential distribution along nonceramic insulators considering the effects of conductors and transmission towers. *IEEE Transactions Power Delivery* 2000; **15**(1):313–318.
7. Asenjo E, Morales N, Valdenegro A. Solution of low frequency complex fields in polluted insulators by means of the finite element method. *IEEE Transactions on Dielectrics and Electrical Insulation* 1997; **4**(1):10–16.
8. Gustavsson T. Outdoor aging of silicone rubber formulations in coastal environment; Licentiate thesis Chalmers University of Technology, School of Electrical and Computer Engineering, Göteborg, Sweden, *Technical report No. 353L*, 2000.
9. Sebestyén Imre. Electric-field calculation for HV insulators using domain-decomposition method. *IEEE Transactions on Power Delivery* 2002; **38**(2):1213–1216.
10. Kontargyri VT, Gonos IF, Ilia NC, Stathopulos IA. Electric field and voltage distribution along insulators under pollution conditions. *Proceedings of the 4th Mediterranean IEE Conference and Exhibition on Power Generation, Transmission, Distribution and Energy Conversion* 2004; Lemesos, Cyprus.
11. Kontargyri VT, Gonos IF, Stathopulos IA, Michaelides AM. Calculation of the electric field on an insulator using the Finite Elements Method. *Proceedings of the 38th International Universities Power Engineering Conference* 2003; Thessaloniki, Greece, 65–68.
12. Michaelides AM, Riley CP, Jay AP, *et al.* Parametric FEA for the design of electric insulating components. *Proceedings of the 3rd Mediterranean Conference on Power Generation, Transmission and Distribution and Energy Conversion* 2002, Athens, Greece.
13. Kontargyri VT, Gonos IF, Stathopulos IA, Michaelides AM. Measurement and verification of the voltage distribution on high voltage insulators. *Proceedings of the 12th Biennial IEEE Conference on Electromagnetic Field Computation* 2006, Maimi, Florida.
14. Hartings R. Electric fields along a post insulator: AC-measurements and calculations. *IEEE Transactions on Power Delivery* 1994; **9**(2):912–918.
15. IEC 60060-1 *High voltage test technique, Part 1: General Definitions and test requirements*; 1989.
16. IEC 60060-2 *High voltage test technique, Part 2: Measuring systems*; 1994.
17. Vector Fields. *OPERA-3d Reference Manual*. Vector Fields Limited: England, 2004.

DOI: 10.1002/etep